Sound propagation and energy relations in churches

Ettore Cirillo and Francesco Martellotta[a)]
Dipartimento di Fisica Tecnica, Politecnico di Bari, via Orabona 4, I-70125 Bari, Italy

(Received 28 January 2005; revised 15 April 2005; accepted 20 April 2005)

The results of an acoustic survey carried out in a group of Italian churches differing in style, typology, and location were used in order to study how the acoustic energy varies inside this kind of space. The effect of different architectural elements on sound propagation was investigated by means of three-dimensional impulse responses measured using a B-format microphone with sweep signals. Side chapels, columns, and trussed roofs appeared to scatter the reflections, so that the purely diffuse exponential sound decay begins after a time interval which grows with the source–receiver distance and with the complexity of the church. The results of the measurements were then compared with predictions given by existing theoretical models to check their accuracy. In particular a model previously proposed by the authors for a specific type of Romanesque churches was further refined taking into account the new findings and making some simplifications. Its application to the wider sample of churches under analysis showed that strength, clarity, and center time can be predicted with reasonable accuracy.
© *2005 Acoustical Society of America.* [DOI: 10.1121/1.1929231]

PACS number(s): 43.55.Br, 43.55.Gx [NX] Pages: 232–248

I. INTRODUCTION

The prediction of acoustical parameters for the purposes of architectural acoustics is a task currently carried out almost exclusively using computer programs. These give detailed and reliable results but require a three-dimensional (3D) model of the room in question. However, researchers and professionals often welcome the availability of simple prediction formulas because they can provide reference values with little calculation effort and also aid the general understanding of room acoustics.

The success of the reverberation time as a measure relies not only on its correlation with perceived subjective quality, but also on its being appropriate for a whole space, and, above all, on its predictability with some simple formulas[1,2] which cover most of the cases (or at least those having even absorption and mixing geometries[3]). When dealing with individual position parameters things become more complex, but, at least for sound strength and clarity, Barron and Lee[4] propose a "revised theory" which, assuming that the reflected sound cannot arrive earlier than direct sound, makes both parameters decrease as a function of the distance. In concert halls and other proportionate spaces this theory provides considerably better predictions of the real behavior of strength and clarity than any classical formula based on constant reverberant field theory.[5] A further modification of this theory has been proposed by Vörlander[6] for reverberant chambers, and this method is commonly used to account for a decrease in reflected level due to sound absorbed at the first reflection.

Unfortunately, several studies show that churches and other places of worship can hardly be included among the "proportionate" spaces. Measurements of both strength and clarity carried out in Gothic-Mudejar churches,[7,8] in Mosques,[9] and in Italian churches[10,11] show that reflected sound levels generally fall below those predicted by the revised theory. Possible explanations for this behavior may be found in the "disproportionate" nature of these kinds of buildings, and in the effect of columns, side aisles, chapels, high vaults, and other architectural elements which scatter or hinder the sound, especially affecting early reflections.[10] However, several works show that, despite some fluctuations, the acoustic parameters under investigation are well related to source–receiver distance, allowing the development of prediction equations based on simple regression models,[12,13] or leading to modifications of the revised theory in order to fit the measured data[7,10] better. However, the model proposed by Sendra *et al.*[7] introduces an attenuation of the reflected energy (based on regression analyses), which equally affects early and late reflections, improving the prediction accuracy for sound level but not for early-to-late energy indices.[8]

The model proposed by Cirillo and Martellotta[10] for Apulian-Romanesque churches assumes that the early reflected energy varies linearly within a time interval proportional to the source–receiver distance, after which the reverberant sound follows a purely exponential decay. The present paper further investigates this model by taking into account a wider group of churches, spanning different architectural styles (from Early-Christian to Modern), and different typologies (basilica plan, single nave, central plan). The whole set of collected data was analyzed in order to validate some of the assumptions on which the modified theory is based. Then, taking into account both the new and the old results, the modified theory was refined in order to remove some of the weakest links. In fact, as observed by Chiles and Barron,[5] the first formulation of the theory requires some approximations that could make its application difficult or, in some ways, subjective. Finally, the reliability of the model was

[a)]Electronic mail: f.martellotta@poliba.it

checked by comparing measured and predicted values of sound strength (G), clarity (C_{80}), and center time (T_s).

II. OVERVIEW OF THEORETICAL MODELS

A. The classical theory

According to the classical theory of sound propagation in enclosed rooms,[1] if the absorption is uniformly distributed and if the sound field is diffuse, the sound pressure level at a point at a distance r from the source (assumed to be omnidirectional) is

$$L(r) = 10 \log\left[\frac{\rho_0 c W}{p_{\text{ref}}^2}\left(\frac{1}{4\pi r^2} + \frac{4}{A}\right)\right] \text{(dB)}, \tag{1}$$

where ρ_0 is the density of the air, c is the sound speed in air, p_{ref} is the standard reference sound pressure, W is the sound power of the source, and A is the total acoustic absorbing area (including both wall absorption and air absorption). A can be expressed as a function of the reverberation time (T) and of the room volume (V) by means of Sabine's equation ($A=0.161\ V/T$). If the sound pressure level is measured in relative terms, that is assuming the level L_{10} of the direct sound at a distance of 10 m from the source as a reference, Eq. (1) becomes

$$G(r) = L(r) - L_{10} = 10 \log(100/r^2 + 31\ 200T/V)\ \text{(dB)}. \tag{2}$$

According to the classical theory, when a perfectly exponential decay follows an interrupted steady-state excitation, then the energy decay after an impulse sound also decays exponentially with the same time constant (equal to $T/13.8$). The instantaneous energy density of the reverberant field following a power impulse $W\cdot\Delta t$ (Δt being the pulse duration) is given by

$$D_r(t) = (W\Delta t/V)\cdot e^{-13.8\cdot t/T}\ (\text{J/m}^3). \tag{3}$$

Consequently, the integral of Eq. (3) divided by Δt equals the steady-state energy of the reverberant sound field generated by a continuous sound source radiating the same power W. The energy density may be conveniently expressed in relative terms by dividing Eq. (3) by the energy density of an impulsive sound at a distance of 10 m:

$$D_{d10} = W\Delta t/(400\pi c)\ (\text{J s/m}^3), \tag{4}$$

so the relative energy density of the reflected sound is

$$g(t) = D_r(t)/D_{d10} = (13.8\cdot 31\ 200/V)\cdot e^{-13.8\cdot t/T}\ (\text{s}^{-1}), \tag{5}$$

and becomes dimensionless after integration. All the energy-based acoustic parameters may be calculated using Eq. (5), but the main drawback of the classical theory is that beyond the reverberation radius the predicted variation in total level and in every other acoustic parameter is small compared to the actual measured values.

B. The revised theory

Barron and Lee[4] proposed a model to account for the larger variations of acoustic parameters observed in real rooms. They noticed that the concert hall situation differed from diffuse requirements in several aspects. However, they found that the sound level decay was linear soon after the direct sound in the majority of the halls, the main discrepancy being observed in the decrease in the reflected sound level with increasing source–receiver distance. So, they proposed a model based on the following assumptions. The direct sound is followed by linear level decay at a rate corresponding to the reverberation time. During a decay the instantaneous level of the late decaying sound is uniform throughout the space, so that decay traces for all receiver positions are superimposed. The time $t=0$ corresponds to the time the signal is emitted from the source, therefore the direct sound reaches a point at a distance r from the source after a time $t_D=r/c$. In this way the integrated energy decreases when the source–receiver distance increases, while the early/late reflected energy ratio remains constant. The integrated value for the reflected sound level is assumed to be, at $t=0$, equal to the value predicted by the classical theory [Eq. (2)].

The application of Barron's revised theory allows the calculation of the integrated relative energy from time t to infinity, given by

$$i(t) = \int_t^\infty g(\Theta)d\Theta = (31\ 200T/V)e^{-13.8t/T}, \tag{6}$$

where Θ is a dummy variable. In order to predict the total sound-pressure level and the clarity index, the sound energy is divided into three components: the direct sound (d), the early reflected sound (from 0 to 80 ms, E_0^{80}), and the late reflected sound (from 80 ms to infinity, E_{80}^{∞}). From Eq. (6), the corresponding energies of each of them become

$$d(r) = 100/r^2, \tag{7}$$

$$E_0^{80}(r) = (31\ 200T/V)e^{-0.04r/T}(1 - e^{-1.11/T}), \tag{8}$$

$$E_{80}^{\infty}(r) = (31\ 200T/V)e^{-0.04r/T}e^{-1.11/T}. \tag{9}$$

So the relative sound level is given by

$$G(r) = 10 \log(d + E_0^{80} + E_{80}^{\infty}), \tag{10}$$

and the clarity index is given by

$$C_{80}(r) = 10 \log[(d + E_0^{80})/E_{80}^{\infty}]. \tag{11}$$

The center time is the first-order momentum of the acoustic energy and, taking into account that for a purely exponential decay the distance of the center of gravity from the origin (i.e., the starting point of the decay t_D) is independent of r and is equal to $T/13.8$, it is given by

$$T_s(r) = T(E_0^{80} + E_{80}^{\infty})/[13.8(d + E_0^{80} + E_{80}^{\infty})]. \tag{12}$$

Barron and Lee compared measured and predicted values, proving the suitability of the revised theory in many concert halls. They remarked, however, that in the presence of highly diffusing ceilings the model tends to overestimate the early energy.

C. The present work ("modified" theory)

The analysis of the results obtained in a group of Romanesque churches[10] showed that the basic hypothesis of the revised theory, namely the uniformity of the reverberant sound field throughout the space, was generally satisfied. However, the time at which the decay began to be linear was later, the farther the measurement position was from the source. Furthermore, at points near the source the early reflections were stronger than the ideal classical reverberant field [as given by Eq. (5)], while, conversely, when the distance from the source grew the early reflections became weaker.

In order to fit with these observations two modifications were introduced. The first one was to assume the reverberant sound field to be uniform, as it is in Barron's theory, but that linear level decay starts with a certain delay (t_R) after the arrival of the direct sound. The measurements showed that this delay was proportional to the source–receiver distance, therefore, in general, it could be written as $t_R=\rho r$. The ρ coefficient depended on the room characteristics and was estimated by assuming that the delay at the farthest point of each room could not exceed the time necessary to have a sufficiently high reflection density. However, the relationship between ρ and the room characteristics was weakened by the arbitrary assumption about the reflection density. Therefore, in order to provide a more reliable and physically acceptable hypothesis based on experimental results, the onset time of the reverberant sound field was investigated as described in detail in the next sections.

The second modification was to schematize the early reflected sound arriving between the direct sound and the reverberant sound field. This part of the sound decay is characterized by discrete reflections which are more or less spaced in time according to the geometry of the room. The magnitude of these reflections is proportional to that of the direct sound according to the characteristics of the room surfaces. In order to simplify the model, the energy of the discrete reflections was schematized by means of a continuous linear function varying from an initial value (at the time t_D), proportional through a factor γ to the energy of the direct sound, and a final value (at time t_D+t_R), equal to the energy of the reverberant field at the same time. The factor γ was introduced to account for two different aspects of the early reflections: their magnitude and their spacing in time.

When a sound hits a wall, part of its energy is absorbed, part is scattered, and the rest is specularly reflected. The first is lost, the second is "distributed" in the space, and the third propagates according to geometrical reflection laws (depending on the wavelength). The first reflections are expected to contain only the fraction of the direct sound energy corresponding to the specularly reflected energy. So, the factor γ was assumed to be proportional to $(1-\alpha)(1-s)$, where α and s are, respectively, the mean absorption coefficient and the mean scattering coefficient of the room surfaces. The estimation of the mean scattering coefficient was the other weakest link of the model due to its mostly subjective assessment. More precise guidelines to estimate this parameter are proposed below on the basis of the results of the present survey.

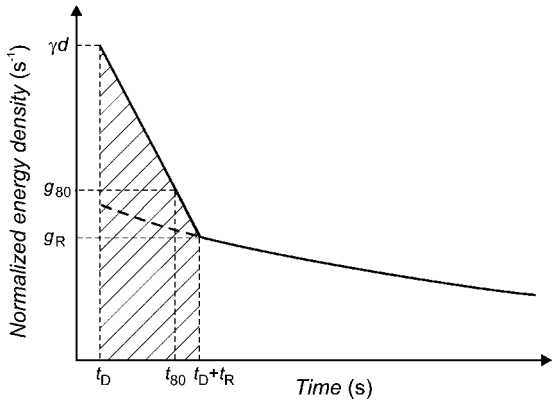

FIG. 1. Plot of the theoretical distribution of energy density of the reflected sound against the time according to the modified theory. The sound is emitted at time $t=0$, and reaches the receiver at t_D. From t_D to t_D+t_R the energy density follows a linear function, and then starts the purely exponential decay.

Finally, the factor γ must be inversely proportional to a time constant in order to transform the energy of the first discrete reflection in a continuous function. The time interval $\Delta\tau$ between the direct sound and the first reflection is actually a complex function of the geometry of the room and cannot be easily calculated. However, as proposed by Vorlander,[6] a reasonable estimate of the average arrival time of the first reflection is given by the time for sound to travel the mean free path equal to $4V/S$, where S is the room surface area. Consequently, $\Delta\tau$ is equal to

$$\Delta\tau = 4V/cS, \tag{13}$$

and the factor γ is given by

$$\gamma = (1-\alpha)(1-s)/\Delta\tau. \tag{14}$$

In order to conclude the definition of the theoretical impulse response, the instantaneous value of the reverberant field energy at the time t_D+t_R was calculated from Eq. (5) expressing the time as a function of the distance:

$$g_R(r) = g(t_D+t_R) = (31\,200\cdot 13.8/V)e^{-(0.04+13.8\rho)r/T}. \tag{15}$$

The resulting theoretical distribution of the energy density impulse response is shown in Fig. 1.

In order to calculate both strength and clarity, it was necessary to integrate the energy contributions previously described. The integrated early reflected energy i_E was calculated as a trapezium area (see Fig. 1), and was given by

$$i_E(r) = t_R(\gamma d + g_R)/2. \tag{16}$$

The integrated reverberant energy was obtained by putting $t=t_D+t_R$ into Eq. (6):

$$i_L(r) = i(t_D+t_R) = (31\,200T/V)e^{-(0.04+13.8\rho)r/T}. \tag{17}$$

Since the direct sound energy d is still given by Eq. (7), the total energy can be calculated by adding d, i_E, and i_L. However, depending on the t_R value, different formulas must be used to calculate the early (E_0^{80}) and late (E_{80}^{∞}) energy with reference to the 80 ms time limit. The simplest method is to

TABLE I. Basic details of the twelve churches surveyed. Reverberation time (T_{30}) is measured at 1 kHz octave band.

Church	Period	Style	Volume (m^3)	Total area (m^2)	Length (m)	T_{30} (s)
St. Sabina Basilica, Rome	432	Early-Christian	17 500	6 000	52	4.1
St. Apollinare in Classe, Ravenna	549	Byzantine	22 500	7 200	57	3.6
Modena Cathedral (Duomo)	1099	Romanesque	20 000	8 000	62	5.0
St. Nicholas Basilica, Bari	1197	Romanesque	32 000	10 500	59	4.4
Lucera Cathedral	1301	Gothic	33 100	10 500	64	5.3
St. Petronius Basilica, Bologna	1390	Gothic	160 000	42 000	130	9.8
San Lorenzo Basilica, Florence	1419	Renaissance	39 000	18 000	82	7.9
The Holy Name of Jesus Church, Rome	1568	Renaissance	39 000	13 000	68	5.1
St. Luke and Martina, Rome	1664	Baroque	8 700	3 500	35	3.1
St. Martin Basilica, Martina Franca	1763	Baroque	16 400	6 500	45	6.9
Concattedrale, Taranto	1970	Modern	9 000	6 200	50	4.2
S. Maria Assunta Church, Riola	1978	Modern	5 500	3 700	35	6.1

calculate E_0^{80} when $t_R > 80$ ms, so that the early reflected energy follows the linear law during the whole interval and, after 80 ms, is equal to

$$g_{80}(r) = \gamma d - 0.08(\gamma d - g_R)/(\rho r). \tag{18}$$

So, the integrated early reflected energy is given by the trapezium area (see Fig. 1):

$$E_0^{80}(r) = 0.08(\gamma d + g_{80})/2. \tag{19}$$

Conversely, when $t_R < 80$ ms, it is the late energy that follows the exponential law throughout the interval and, consequently E_{80}^{∞} may be expressed using Eq. (9).

In this way when $t_R > 80$ ms, E_0^{80} is given by Eq. (19) and $E_{80}^{\infty} = i_E + i_L - E_0^{80}$, when $t_R < 80$ ms then E_{80}^{∞} is given by Eq. (9) and $E_0^{80} = i_E + i_L - E_{80}^{\infty}$. Consequently G and C_{80} may be calculated as usual by means of Eqs. (10) and (11), while the center time requires a different formula to take into account the modified early energy (Fig. 1). The trapezium may be divided into a square having area $g_R \cdot t_R$, centered at $t_R/2$, and a triangle having area $(\gamma d - g_R) \cdot t_R/2$, centered at $t_R/3$. The center of the late energy is, again, at $T/13.8$ after the starting point (which, this time, is t_R). So the first-order momentum yields

$$T_s(r) = \lfloor (\gamma d/2 + g_R) t_R^2/3 + (t_R + T/13.8) i_L \rfloor / (d + i_E + i_L). \tag{20}$$

III. THE ACOUSTIC SURVEY

A. The churches surveyed

Twelve Catholic churches were analyzed during the present survey. Churches of different period and geographic area were included in the survey in order to have a sample varying in architectural style, typology, and dimensions, as reported in Table I and Fig. 2. All the churches were unoccupied during the measurements and their floors were only covered with pews (and sometimes groups of seats) according to the layout reported in Fig. 2. Pews were made of wood and in none of the cases were covered with cushions or any other absorbing material. Only in few cases [Figs. 2(c), 2(f), and 2(k)] large floor surfaces near the altar were covered with carpets. A short description of the churches surveyed is provided below.

Santa Sabina Basilica [Fig. 2(a)] is an Early-Christian church built at the beginning of the fifth century. It has a basilica plan with a large apse. The nave is covered with a flat wooden ceiling, while the side aisles are roofed. The walls are flat and finished in plaster.

St. Apollinare in Classe [Fig. 2(b)] is a Byzantine church, with a basilica plan without transept and with a large apse. Both the nave and the aisles are covered with a trussed roof. The walls are flat and decorated with mosaics, and the chancel area is raised about 1 m above the floor.

Modena Cathedral [Fig. 2(c)] is a Romanesque church with a basilica plan without transept and with three apses. The walls and the cross-vaults that cover both the nave and the aisles are made of brick and are smooth. The chancel area was, originally, located above the crypt which communicates with the main volume of the church by means of wide openings. Nowadays the altar is located in front of the crypt in the main nave.

St. Nicholas Basilica in Bari [Fig. 2(d)] is the prototype of the Apulian Romanesque style, it has a transept with three apses. Two columns separate the transept and the nave. There are roofed women's galleries, while the nave ceiling is wooden with large painted canvases. The side aisles are cross-vaulted.

Lucera Cathedral [Fig. 2(f)] is a large church built in Angevine-gothic style. It has a cross-shaped plan with a transept and three apses. The high nave and the aisles are covered with a wooden roof with trusses. The walls and the apses are finished in plaster, while the columns are made of rough stone.

St. Petronius Basilica [Fig. 2(e)] in Bologna is the fifth largest church in the world. It is built in gothic style, even though it was completed in the renaissance period. The church has a central nave (which terminates with an apse in the choir), with aisles and deep chapels. The high cross-vaults (more than 40 m) that cover the nave, and those covering the aisles and the chapels are plastered, as are the walls, while the ribbed columns are made of bricks.

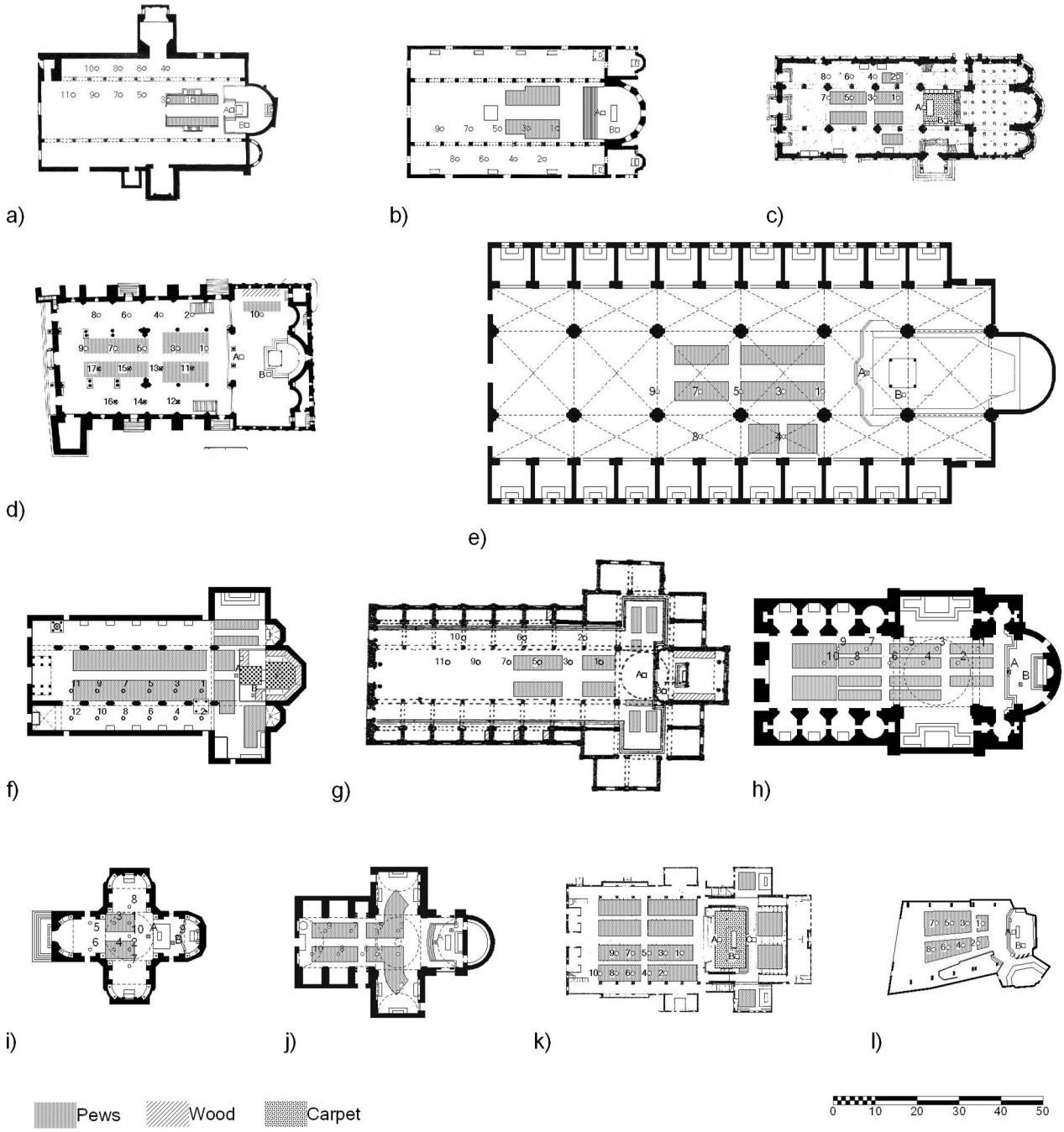

FIG. 2. Plans of the twelve churches surveyed: (a) Santa Sabina Basilica in Rome, (b) St. Apollinare in Classe, (c) Modena Cathedral, (d) St. Nicholas Basilica in Bari, (e) St. Petronius Basilica in Bologna, (f) Lucera Cathedral, (g) San Lorenzo Basilica in Florence, (h) The Holy Name of Jesus in Rome, (i) St. Luca e Martina in Rome, (j) St. Martin Basilica in Martina Franca, (k) Concattedrale of Taranto, (l) S. Maria Assunta in Riola. (Same scale for all the churches.)

San Lorenzo Basilica in Florence [Fig. 2(g)] was built between 1419 and 1470 by Brunelleschi. It has a cruciform plan, with the main nave and the transept covered with a flat wooden ceiling and side aisles covered with vaults. The walls are flanked by chapels. The walls are scarcely decorated and are finished in plaster.

The church of the Holy Name of Jesus in Rome [Fig. 2(h)] was built in the late Renaissance style by Jacopo da Vignola. The church has a Latin-cross plan, with a dome over the crossing and barrel vaults to cover the nave and the transept braces. Chapels flank the main nave. The walls and the vaults are covered with decorations and paintings.

The church of the Saints Luca and Martina in Rome [Fig. 2(i)] was built in 1635–1664 by Pietro da Cortona as a domed cruciform church, according to the Baroque style. The walls and the vaults are finished in plaster and richly decorated.

St. Martin Basilica in Martina Franca [Fig. 2(j)] was built from 1747 to 1763 in baroque style. The church has a single nave with a large transept with a dome above the crossing. The nave is covered with a barrel vault and flanked by deep chapels. Walls and vaults are finished in plaster and abundantly decorated.

The Cathedral of the Blessed Virgin Mary in Taranto

[Fig. 2(k)], also known as the "Concattedrale," was built in 1970 by Giò Ponti. The church has a large nave with narrow aisles. The ceiling is flat with beams and is finished in rough plaster, as are the walls. The chancel area is raised and is covered by a higher ceiling. The floor area is tightly fitted with wooden pews.

The church of Our Lady Assumed into Heaven in Riola [Fig. 2(l)] was designed by Alvar Aalto in 1966 and completed in 1978. The church is an asymmetrical room (nearly fan-shaped) with an asymmetrical vault supported by concrete arches. The walls and the vault are finished in smooth plaster.

B. Measurement technique

The measurements were carried out using an omnidirectional sound source made of twelve 120 mm loudspeakers (with a flat response up to 16 kHz) mounted on a dodecahedron, together with an additional sub-woofer to cover the frequencies from 40 to 100 Hz. A calibrated measurement chain made by a GRAS 40-AR omni-directional microphone together with a 01 dB Symphonie system was used to measure the sound pressure levels. A MLS signal was used to get the calibrated impulse responses to obtain the strength values. The other acoustic parameters were obtained using high-quality impulse responses collected using a Soundfield Mk-V microphone, an Echo Audio Layla 24 sound card, and a constant envelope equalized sine sweep[14] to excite the room.

Two source positions were used in each church, one on the axis of symmetry and one off the axis, both in the chancel area. The source was placed 1.5 m above the floor. Nine receiver positions were used on average. In very large but symmetrical churches the receivers were only placed in one half of the floor, otherwise they were spread to cover the whole floor area uniformly (Fig. 2). The microphone was placed 1.2 m from the floor surface.

All the measurements and the calculations of the indices were carried out according to ISO-3382 standard.[15] In particular for the measurement of the sound strength (G) the sound power of the source was calibrated in a reverberation chamber, employing the same measurement chain and the same settings used during the on site survey. For the sake of brevity, in the following analysis only 1 kHz octave band results are presented.

IV. EXPERIMENTAL RESULTS

A. Spatial distribution of sound levels

The measurements of the relative sound level performed in the churches surveyed showed that the level decreases as a function of the source–receiver distance. However, in agreement with the results shown in other works,[7,9–11] the decrease appears steeper than it is in auditorium spaces and the like. So the agreement with the revised theory is also quite unsatisfactory. In particular, the mean values are predicted with acceptable accuracy (with a mean error of 0.6 dB, and a maximum error of 1.2 dB), but the predicted rate of decay is generally lower than measured (by about 1 dB/10 m), underestimating the values near the source, and overestimating the values far from the source (Fig. 3). At this level of investigation it cannot be stated whether the level decay depends on weaker late reflections, or, more likely, on a lack of early reflections. In order to better understand this issue, the time distribution of the reflections must be taken into account.

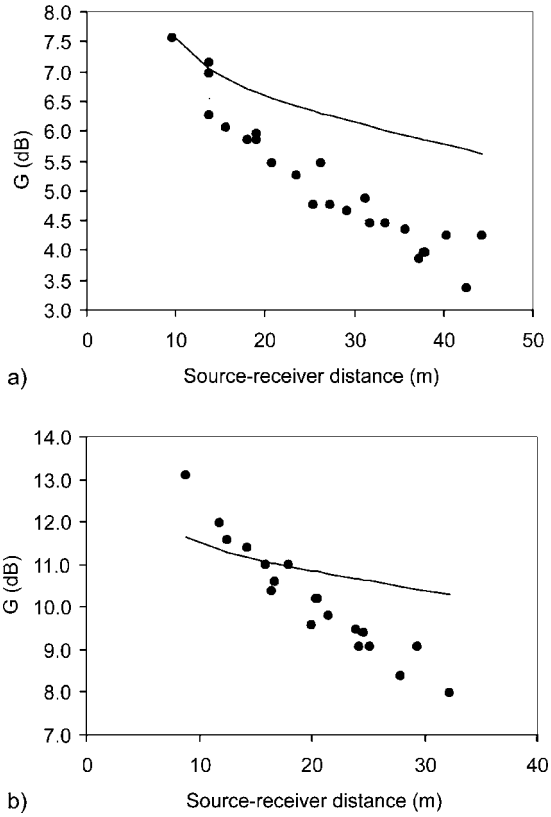

FIG. 3. Plot of measured (●) and Barron's (—) values of the relative sound level at 1 kHz octave inside Lucera Cathedral (a), and the Concattedrale in Taranto (b).

B. Spatial distribution of early and late sound

The first approach to investigate the time distribution of the reflections was the analysis of the early and late reflected levels assuming 80 ms as the time limit between the early and late part. Figure 4 shows that the early sound (from 5 to 80 ms) is quite scattered, proving its strong dependence on single reflections. However, the correlation with source–receiver distance is significant and points out a clear decreasing trend with a rate of decay higher than that predicted by the model. This means that the reflections arriving at the farthest receivers within 80 ms are both few and weak. The late reflected level is less scattered but again shows a decreasing trend with a slope steeper than that predicted by the model. This lack in energy at the farthest points can be explained by taking into account that early reflections continue to arrive well after the 80 ms limit, with a weaker energy and a smaller density than predicted by the classical theory.

Evidence supporting this hypothesis comes from the plot of the early and late reflected levels when assuming a time limit of 500 instead of 80 ms. After this time the late reflections should behave reasonably in a purely statistical (i.e., diffuse) way, and the agreement with predicted values should be better. Figure 5 confirms this, showing a good match be-

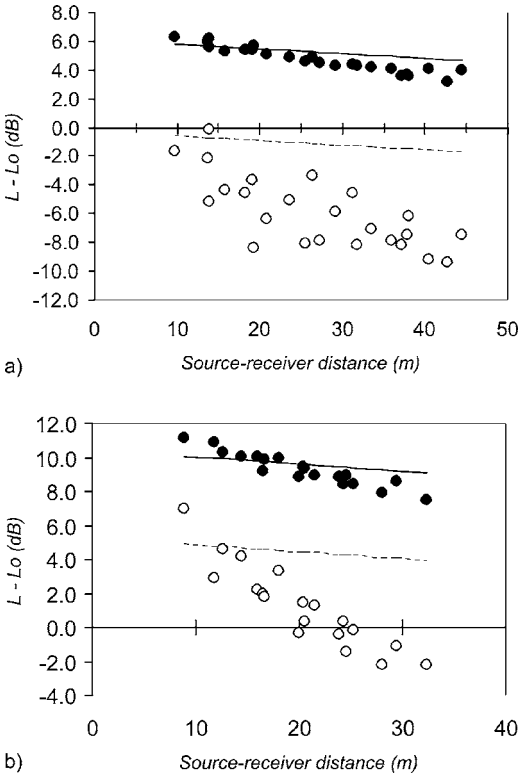

FIG. 4. Plot of predicted (using Barron's model) and measured early and late reflected sound level at 1 kHz octave against the source–receiver distance for Lucera Cathedral (a), and the Concattedrale in Taranto (b). (●) Measured late level, (○) measured early sound level, (—) predicted late sound level, (---) predicted early sound level. Early–late limit is assumed at 80 ms and direct sound is excluded.

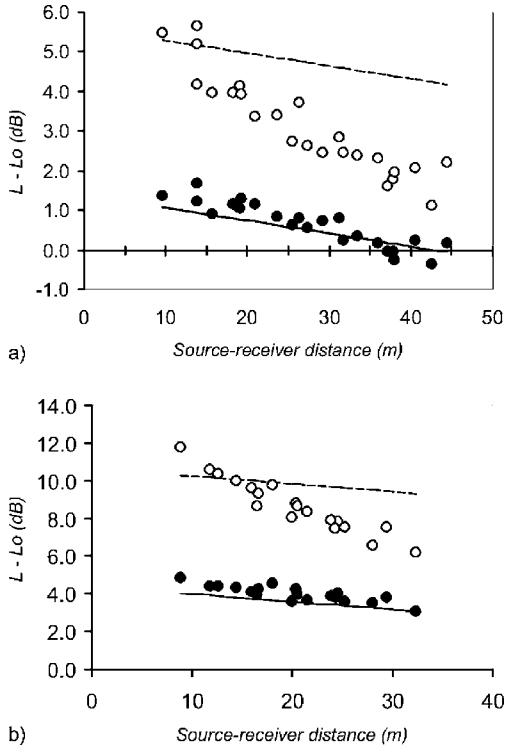

FIG. 5. Plot of predicted (using Barron's model) and measured early and late reflected sound level at 1 kHz octave against the source–receiver distance for Lucera Cathedral (a), and the Concattedrale in Taranto (b). (●) Measured late level, (○) measured early sound level, (—) predicted late sound level, (---) predicted early sound level. Early–late limit is assumed at 500 ms and direct sound is excluded.

tween measured and predicted late levels, while the early level decreases almost linearly with a greater slope than predicted.

Further evidence of the late transition to the purely reverberant sound field comes from analyzing the early decay traces relative to receivers at different distances from the source (Fig. 6). According to the revised theory the instantaneous level must be the same at all positions during a sound decay. Therefore the measured sound decay should coincide, provided that $t=0$ is the time at which the sound is emitted and the relative levels are taken into account when plotting the decay curves. Figure 6 shows that the starting point of each decay can be identified quite clearly and depends on the effective source–receiver distance. The early reflections appear soon after the direct sound as the more or less evident steps following the direct sound. After a certain time the curves converge, showing the later reflected sound to be reasonably uniform throughout the space. It can be seen that perfect convergence is hardly obtained. However, the convergence point, assumed to be the time at which all the decay curves are aligned and the following decay is linear, can be quite easily detected by visual inspection and appears only about 0.5 s after the direct sound.

C. The directional characteristics of the early reflections

The analysis of the early and late part of the reflected sound showed that the critical point of the application of Barron's model to the churches is represented by the prediction of the early reflected energy. In fact, taking into account only the late reverberant sound (arriving at least 0.5 s after the direct sound) the agreement between the measurements and the model is good. On the contrary, the same analysis pointed out that there is a clearly distinct early part where, depending on the energy and on the density of the reflections arriving, the integrated energy may be higher or lower than predicted. Figures 4 and 5 clearly show that the closer the receiver to the source, the stronger the reflections, and vice versa, with the early reflections becoming weaker as the source–receiver distance grows.

This behavior is due, according to Barron and Lee,[4] to highly diffusing surfaces which reflect the sound energy in nonspecular directions so that, on average, they act according to Lambert's Law, sending less energy to the rear of the room (far from the source) than to the front. In the surveyed churches there are trusses on the roof, cross-vaults, columns along the nave, niches or deeper chapels, and other architectural elements which scatter the incident sound and might lead to the observed behavior.

This hypothesis can be verified by taking advantage of the three-dimensional (3D) impulse responses obtained using the B-Format recording technique. The directional components (X,Y,Z) were combined with the omni-directional component (W) to provide a 3D impulse response. Polar plots representing the energy content arriving from discrete directions represented by azimuthal and zenithal angles projected on the same plane were used to make the information

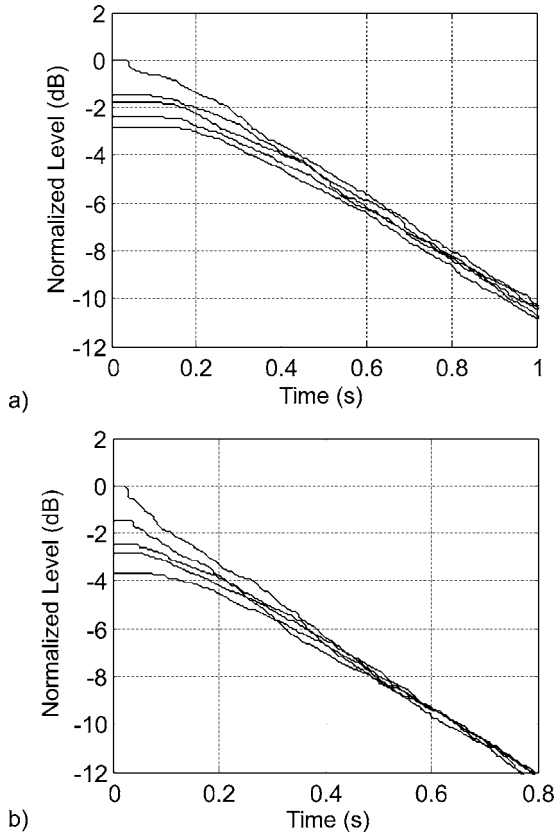

FIG. 6. Early decay traces at 1 kHz octave, measured in different points of the nave of (a) Lucera Cathedral, and (b) the Concattedrale in Taranto. Sound is emitted is $t=0$ on the time axis.

more easily accessible. Then, in order also to take the time distribution into account, three time slices were considered: from 5 to 80 ms (so excluding the direct sound), from 80 to 500 ms, and from 500 to 1000 ms. For each plot the level of the reflections was normalized by assuming the maximum energy value for that slice as a reference.

A quantitative measure which can be conveniently used in this analysis is the directional diffusion δ, defined, for each time slice, as:[1,16]

$$\delta = (1 - \mu/\mu_0) \times 100\% \tag{21}$$

with μ computed from

$$\mu = \frac{1}{\bar{e}} \sum |e_i - \bar{e}|, \tag{22}$$

where e_i is the energy content associated to the direction i, and $\bar{e}$ is the mean energy over all directions. The quantity μ_0 is the value for single plane wave incidence and depends on the number of subdivisions, so δ can vary between 0% (anechoic) to 100% (isotropic). In the present case δ was calculated with reference to the horizontal/azimuthal distribution (δ_h) and to the vertical/zenithal distribution (δ_v).

Figure 7 reports the polar plots for a representative sample of churches. In order to make coherent comparisons only the farthest points from the source were considered, and in all the cases the source was at the center of the chancel.

In the first case, the church of St. Apollinare in Classe, the reflections arriving within 80 ms are scarcely diffuse ($\delta_h=65\%$, $\delta_v=65\%$), and come mostly from the front, probably because of the flat and reflecting surfaces of the chancel. The effect of the highly diffusing ceiling is particularly evident in the lack of strong early reflections from the top. In fact, there are mostly frontal reflections until 500 ms, even though the diffusion is increased. The later part presents diffuse reflections ($\delta_h=91\%$, $\delta_v=81\%$) coming quite evenly in the horizontal plane, and with a prevalence from above (due to the microphone position) in the vertical plane.

In the second case, Modena Cathedral, the naves are covered with cross vaults instead of a wooden roof. From 5 to 80 ms the sound comes mostly from the front-top quadrant and is scarcely diffuse ($\delta_h=59\%$, $\delta_v=56\%$), also because of a strong lateral reflection. From 80 to 500 ms the reflections are more evenly distributed even though they appear to be mostly lateral on the horizontal plane, while in the vertical plane there is a certain dominance of purely perpendicular reflections probably because the chancel area is unable to reflect the sound. In fact, the late reflections are clearly diffuse in the horizontal plane ($\delta_h=90\%$), while on the vertical plane the reflections keep on coming quite perpendicularly from the top ($\delta_v=75\%$). In this case the cross-vaults are wide (due to the large span of the nave) and not very high, so they behave in a mixed mode, partly scattering the sound (when the curvature is perpendicular to the nave), and partly reflecting it (when the curvature is parallel to the nave).

In the third case, the church of the Holy Name of Jesus, the barrel vault provides strong reflections from the front-top quadrant until 500 ms. The early reflections are scarcely diffuse ($\delta_h=59\%$, $\delta_v=56\%$), and even the reflections arriving between 80 and 500 ms are less diffuse than in other churches because of a lack of lateral reflections. In fact, the side walls, due to their decorations and deep chapels, scatter and absorb the sound almost completely so that the lateral reflections are very weak compared to those from the front. After 500 ms the sound field becomes diffuse ($\delta_h=90\%$, $\delta_v=74\%$) but on the vertical plane the behavior is similar to Modena, with reflections coming almost perpendicularly from the top.

In the last case, the church in Riola, the very early reflections are weakly diffuse ($\delta_h=52\%$, $\delta_v=44\%$), and come mostly from the front-top quadrant due to the large reflecting surfaces that surround the source. However, soon after, the sound field becomes nearly diffuse ($\delta_h=91\%$, $\delta_v=81\%$) with an almost uniform distribution of the reflections from the sides and from the top.

The analysis of the directional characteristics of the early reflections shows that the depth and the decorations of the side chapels strongly affect the lateral energy because the sound is reflected according to complex paths that prevent the sound from coming back into the nave. A comparable effect, although not so dramatic, is due to side aisles and decorated walls that reduce the lateral reflections, making them weaker and scattered, as if the surface acted according

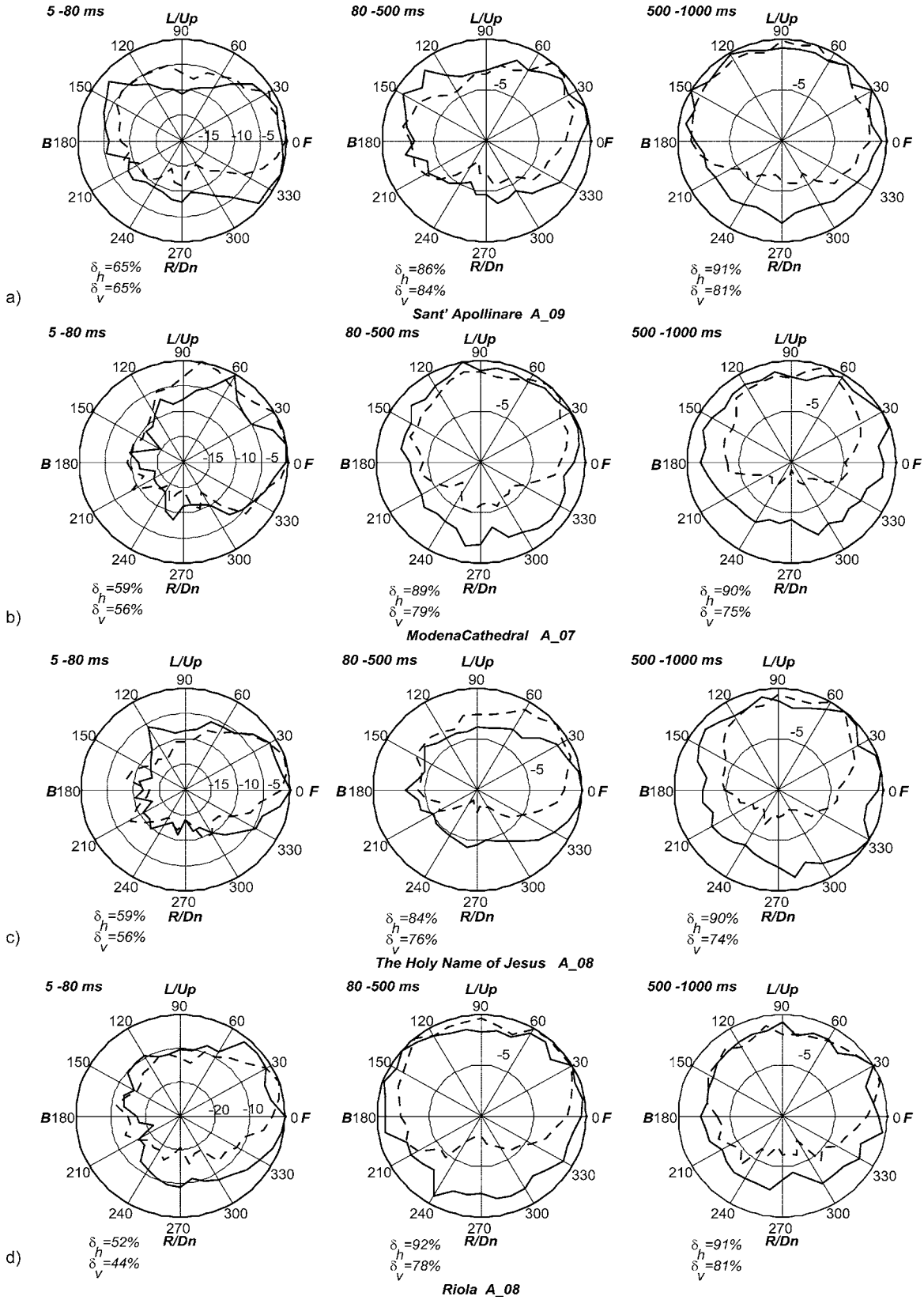

FIG. 7. Polar plots of the directional distribution of the energy content of the reflections at 1 kHz. Reflection levels are normalized with reference to the maximum energy content for each time slice. (---) Energy level in the vertical plane; (—) energy level in the horizontal plane.

to Lambert's law. Similar behavior is observed in the vertical plane in the presence of trussed roofs and highly diffusing ceilings, while vaults, especially barrel vaults, provide stronger reflections.

D. The time distribution of the early reflections

The scattering of early reflections observed in the previous section is also responsible for the slower build up of the

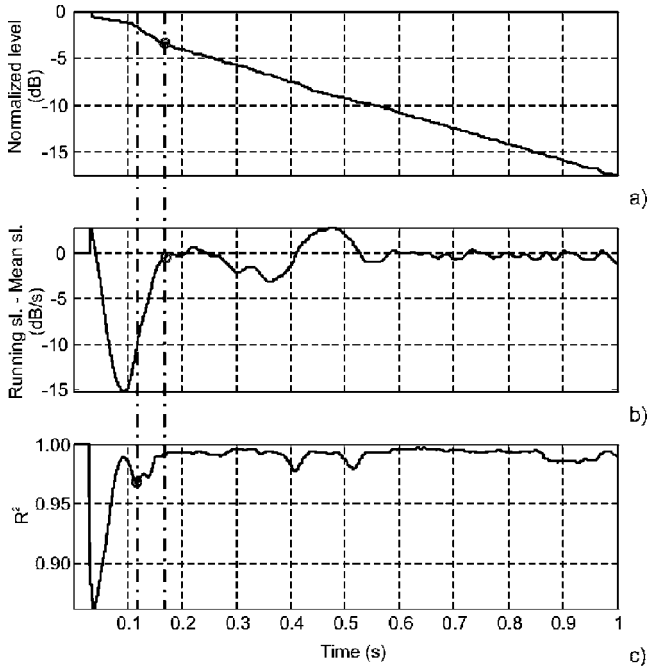

FIG. 8. Example of calculation of the onset time of the reverberant sound field. (a) Plot of the decay curve; (b) plot of the difference between running slope calculated over a 100 ms interval and mean slope; (c) plot of the correlation coefficient of the best fit line.

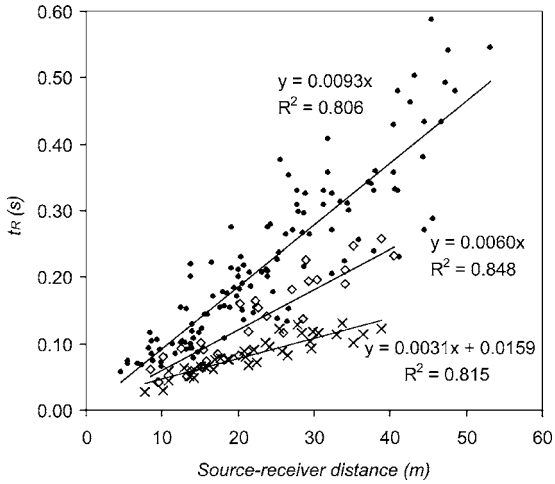

FIG. 9. Scatterplot of the onset times as a function of the source–receiver distance. (×) Simple shape churches (Santa Sabina, Sant'Apollinare, and Riola); (◇) basilica-plan churches (Modena Cathedral, St. Nicholas Basilica); (●) complex shape churches.

purely reverberant sound field. In fact, it was observed that in most of the cases the sound appeared fully diffuse only after 500 ms (Fig. 6). However, this value is the time limit after which all the decay curves became linear, so it cannot be excluded that it might be shorter in some cases. It can be reasonably supposed that the onset time of the reverberant sound field might be room-dependent and, inside each church, position-dependent. In order to investigate this hypothesis the onset time of the reverberant sound was determined by means of the running slope of the level decay curves.

The running slope at time t was defined as the slope of the best-fit line calculated over the 100 ms portion of the decay curve following t. The determination coefficient R^2 of the best-fit line was also calculated, because lower values may easily indicate the presence of steps or sudden slope changes in the decay curve. The onset time was finally assumed to be the time at which the running slope equals for the first time the mean slope of the decay curve (based on T calculation), provided that R^2 shows a relative minimum shifted (ideally) 50 ms earlier (Fig. 8), meaning that the slope is actually changing.

The whole set of the onset time values was plotted as a function of the source–receiver distance, as this was the simpler and more significant parameter to describe individual position differences. The plot, reported in Fig. 9, shows that the correlation between the onset times and the distance is good, provided that three different subsets of data are considered. The subsets were obtained by grouping all the onset times belonging to churches showing the same trend on the plot. In all the cases, the best regression models proved to be linear (as can be confirmed by a simple visual inspection of the plot). In addition, in order to avoid equations yielding negative t_R values, in two cases the regression lines were forced by the origin at the expense of a slightly worse correlation coefficient. The first group included the churches of Santa Sabina, Sant'Apollinare in Classe and the parish church in Riola. The regression line was statistically significant ($R^2=0.815; p=0.05$), and its equation was $t_R=0.0031r+0.0159$. The second group included St. Nicholas Basilica ad Modena Cathedral. The regression line was statistically significant ($R^2=0.848, p=0.05$), and its equation was $t_R=0.0060r$. The third group included all the other churches and showed some scatter of the data but, thanks to the large number of observations, the regression line had the highest statistical significance ($R^2=0.806, p=0.03$), and its equation was $t_R=0.0093r$.

The above-presented results confirm that, as proposed by Cirillo and Martellotta,[10] the onset time of the reverberant field depends on the source–receiver distance. However, the identification of a group of linear equations valid for a range of churches, suggests a simpler dependence on the room characteristics than was originally proposed. In fact, the churches of the first group share large flat reflecting surfaces and simple geometries, while the churches in the third group share complex volume articulation. So it can be reasonably supposed that the coefficient of proportionality between t_R and r might be simply chosen as a function of the general room characteristics.

A further interpretation of the results may be obtained by expressing t_R as a function of the direct sound delay t_D. For the first group of churches the equation becomes $t_R=1.06\cdot t_D+0.016$, for the second it becomes $t_R=2.06\cdot t_D$, and for the third it becomes $t_R=3.19\cdot t_D$. According to the equations reported the ratio t_R/t_D should be constant in each church, but the spread of the data reported in Fig. 9 suggests that there might be significant fluctuations. The mean ratio t_R/t_D was calculated for each church together with the standard deviation of the individual position values. The results, reported in Table II, show that the mean values for each church do not differ much from the group values and, above all, the standard deviations are relatively small and vary be-

TABLE II. Mean values of the onset time t_R and of the ratio t_R/t_D.

Church	t_R/t_D	
	Mean	St. Dev.
S. Sabina Basilica, Rome	1.45	17%
St. Apollinare in Classe	1.24	16%
Duomo of Modena	1.90	26%
St. Nicholas Basilica, Bari	2.13	24%
St. Petronius Basilica	2.84	26%
Lucera Cathedral	3.54	28%
San Lorenzo Basilica, Florence	3.25	18%
Jesus Church, Rome	2.97	21%
St. Luca and Martina, Rome	3.30	28%
St. Martin Basilica, Martina Fr.	2.99	19%
Concattedrale, Taranto	3.42	16%
S. Maria Assunta, Riola	1.48	21%

tween 16% and 28%. In addition, the values of t_R/t_D show no specific trend and no significant correlation with the distance, confirming that the hypothesis of a constant t_R/t_D for a given church is reasonable.

Further evidence of the reliability of this hypothesis can be obtained by plotting predicted and measured late levels assuming the onset time of the reverberant sound to be proportional to t_D according to the values reported in Table II.

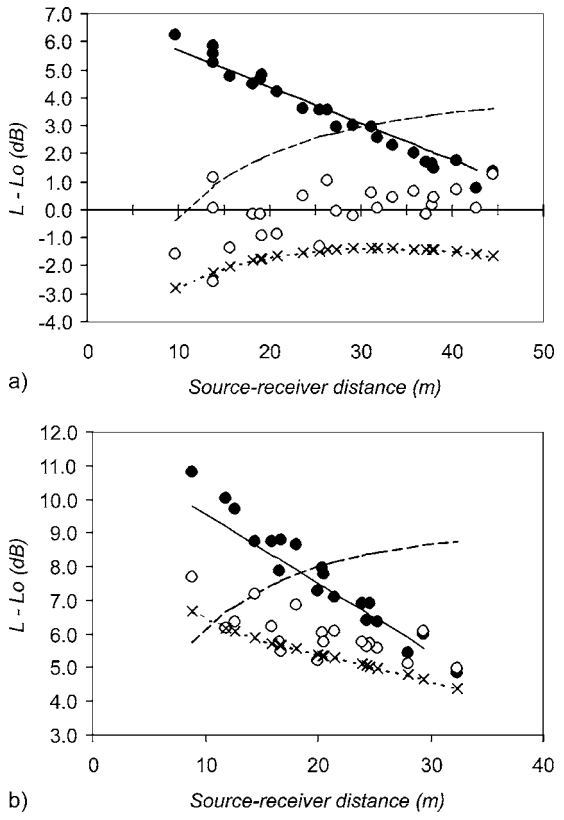

FIG. 10. Plot of predicted (using Barron's model) and measured early and late reflected sound level at 1 kHz octave against the source–receiver distance for Lucera Cathedral (a), and the Concattedrale in Taranto (b). (●) Measured late level, (○) measured early sound level, (—) predicted late sound level, (---) predicted early sound level, (-×-) early sound level predicted using the modified theory. Early–late limit is assumed proportional to the direct sound delay.

The plot, reported in Fig. 10, shows that the agreement between the late levels is as good as that observed in Fig. 5, where a constant t_R was assumed. Predicted and measured values of the early levels are significantly different. However, due to the importance of the early reflections this issue is discussed in detail in Sec. IV E.

E. The energy of the early reflections

In the previous sections the early reflections were analyzed both in terms of directional properties, and of time distribution. This allowed better understanding of the effect of highly scattering room surfaces, which produce weaker early reflections and cause a slower build up of the purely reverberant sound field. However, no information was obtained about the intensity of the early reflections. Some clues can be obtained by comparing Figs. 4, 5, and 10. Figure 4 reports the early reflection level assuming 80 ms as the time limit, here there are the largest variations, with the level decreasing rapidly as the distance grows, showing that at the farthest points the reflections arriving within 80 ms are both few and very weak. Figure 5 assumes a longer time limit of 500 ms, showing that the early level still decreases as the distance grows but the slope is smaller than before. This behavior can be explained by taking into account the hypothesis that t_R is proportional to t_D. In fact, a constant t_R would imply that at points near the source a part of the reverberant energy is included in the early interval, so that measured values appear more stable and similar to predicted ones and the contribution of the exponential decay becomes weaker at points far from the source. Finally, Fig. 10 shows the early level calculated assuming a variable time limit (proportional to t_D, according to the values reported in Table II). Here the data show, in one case, a tendency to grow with distance with an asymptotic trend, and in the other a tendency to decrease with distance. Figure 11 explains this, showing that in Lucera Cathedral at points near the source there was a lack of reflections within the first 50–100 ms after the direct sound so that the level of the integrated sound increases as the distance, and hence the time interval, grows. On the contrary in the Concattedrale the first reflections were stronger (their intensity is virtually the same as the direct sound), and their decrease as a function of the distance determines the behavior observed in Fig. 10.

An observation that supports the proposed modification to Barron's model is that between the direct sound and the onset of the reverberant sound the energy density appears to vary, with some unavoidable fluctuations, according to a linear function starting from the energy density of the very first reflection and ending with the energy of the reverberant field (Fig. 11).

V. REFINING THE MODEL

When the "modified theory" was presented in Sec. II D two aspects were left open. The first was the estimation of the coefficient ρ required to define the onset time of the purely reverberant sound field, and the second was the estimation of the mean scattering coefficient s necessary to define the energy of the early reflections.

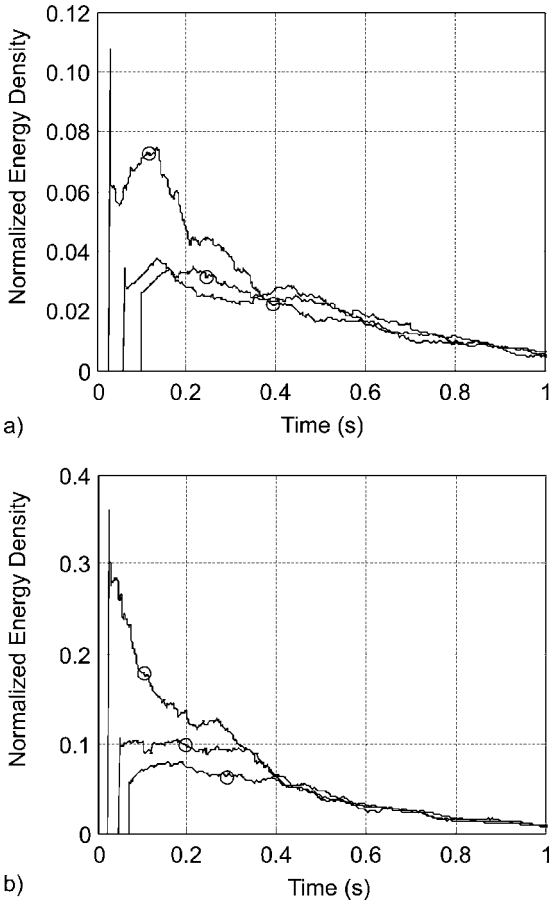

FIG. 11. Plot of the energy density at 1 kHz octave for Lucera Cathedral (a), the Concattedrale in Taranto (b). Circles correspond to the early–late limit assumed proportional to the direct sound delay.

The analysis of the experimental results reported in Sec. IV showed that the onset time of the purely reverberant sound field t_R could be reasonably assumed to be proportional to the direct sound delay t_D. The proportionality factor, given by the ratio t_R/t_D, was reported for each church in Table II, showing that the values varied in a relatively narrow range from 1.24 to 3.54. However, the analysis of the whole sample of data showed that the churches could be divided into three groups with t_R/t_D ratios equal to 1.06 for churches having a simple shape, 2.06 for churches having a proportionate basilica plan, and 3.19 for churches having disproportionate shapes and strongly diffusing surfaces. Finally, in order to make the choice of the ρ values easier and less arbitrary, the three t_R/t_D ratios were rounded to the nearest integer and assigned to a specific set of architectural features according to the classification reported in Table III. According to this classification, the revised theory may be considered as a the limiting case in which ρ equals zero.

The definition of the mean scattering coefficient s cannot rely on measured experimental data because the early reflections depend on such a large number of factors as to prevent any extrapolation of the individual contribution of the scattering. However, some considerations on the propagation of the sound from the sources to the receivers may help in defining a set of suitable values for the scattering coefficient. First of all, it is reasonable to assume that the most important

TABLE III. Values of ρ according to the architectural typology.

Architectural typology	$k=t_R/t_D$	$\rho=k/c$
Auditorium-like churches and churches with large reflecting surfaces and small chancel area	1	0.029
Typical basilica-plan churches, with transept, side aisles, columns, and diffusing ceiling or roof	2	0.058
Basilica-plan churches with very high ceiling and churches with strongly scattering surfaces (deep side aisles or lateral chapels)	3	0.087

contribution to the early reflections is given by the surfaces near the source and near the receivers. The receivers are, in most of the cases, distributed in the church according to a standardized pattern so that they are far from strongly reflecting surfaces, apart from the floor which is generally covered with pews or chairs (in fact, the polar distribution of the reflections reported in Fig. 7 clearly shows that both the early and late reflections rarely come from the bottom). Consequently, the scattering coefficient is mostly dependent on the characteristics of the "sending end" (i.e., the chancel area) of each church, and may be defined in order to include other effects not strictly dependent on scattering. The elements which may influence the scattering of sound are the height of the chancel (that reduces the risk of interference due to grazing propagation), the presence of flat reflecting walls and their distance from the source, and the presence of obstacles between the source and the receivers (such as rails and columns which may hinder the propagation toward given directions). According to these considerations a set of values associated to four groups of chancel typologies, as reported in Table IV, was proposed in order to provide a simple criterion to choose the scattering coefficient.

In this way all the parameters required to apply the new model may be easily calculated or assigned provided that the architectural features of the church are known.

VI. VALIDATION OF THE MODEL

The modified theory was finally applied to the churches surveyed in order to be validated. The geometrical data (such as volume, surface area, etc.) were used together with the reverberation time (see Table I) to determine the coefficients α and $\Delta\tau$, while s and ρ resulted from the classifications reported in Tables III and IV. A summary of the additional parameters used to apply the modified theory in each church is reported in Table V. Then, for each church, the early and

TABLE IV. Values of the mean scattering coefficient according to the chancel typology.

Chancel typology	s
Raised, or bounded by very close hard, flat surfaces	0.20
Slightly raised, bounded by relatively flat reflecting walls with few obstacles between source and walls	0.40
Very slightly raised, bounded by scattering (decorated) walls with some obstacles between source and walls	0.60
Not raised, bounded by far reflecting walls and full of scattering furniture	0.80

TABLE V. Summary of the values required by the new model for each church surveyed.

Church	MFP (m)	$\Delta\tau$ (ms)	α	s	γ (s^{-1})	ρ (s/m)	t_R/t_D
S. Sabina Basilica, Rome	11.7	34	0.11	0.40	5.2	0.0029	1.0
St. Apollinare in Classe, Ravenna	12.5	36	0.14	0.20	18.9	0.0029	1.0
Modena Cathedral	10.0	29	0.08	0.60	12.6	0.0058	2.0
St. Nicholas Basilica, Bari	12.2	36	0.11	0.60	10.0	0.0058	2.0
St. Petronius Basilica, Bologna	15.2	44	0.06	0.20	16.9	0.0087	3.0
Lucera Cathedral	12.5	36	0.09	0.80	5.0	0.0087	3.0
San Lorenzo Basilica, Florence	8.7	25	0.04	0.40	22.7	0.0087	3.0
The Holy Name of Jesus Church, Rome	12.0	35	0.09	0.40	15.5	0.0087	3.0
St. Luca and Martina, Rome	9.9	29	0.13	0.60	12.0	0.0087	3.0
St. Martin Basilica, Martina Franca	10.1	29	0.06	0.20	25.6	0.0087	3.0
Concattedrale, Taranto	5.8	17	0.06	0.20	44.6	0.0087	3.0
S. Maria Assunta Church, Riola	11.0	20	0.07	0.20	23.1	0.0029	1.0

late levels defined assuming t_R as the early/late limit, as well as the values of G, C_{80}, and T_s were calculated for every source–receiver combination using both the revised and the modified theory. The results of the calculations were then compared with the data measured in each church by means of four indices: the difference between mean values, the *just noticeable difference* (JND), the prediction accuracy, and the slope difference. The JND was estimated as the mean ratio between the mean absolute difference between measured and predicted values in each source–receiver combination, and the difference limen for the given parameter. The difference limens commonly adopted for the selected parameters are 1 dB for both G and C_{80}, and 10 ms for T_S.[17,18] The prediction accuracy was estimated by the mean rms error between measured and predicted values for each source–receiver combination. Finally, linear regressions for parameter values against the source–receiver distance were performed and the difference between the measured and predicted values of the slopes was determined. Mean values were calculated excluding the cases where the correlations were not significant at the 5% level.

A. Early and late sound

The first test of the reliability of the new model is the analysis of the early and late components of the reflected sound defined under the assumption of a t_R proportional to t_D. In particular Fig. 10 showed that this hypothesis allows a better estimation of the purely reverberant sound field. Table VI reports the difference between mean values, the rms error, and the slope difference for both early and late reflections. It can be observed that the agreement between the measured and predicted late levels is good, with a mean rms error of 0.57 dB, and a mean slope difference of −0.41 dB/10 m which confirms that, despite the modifications, the theory still tends to underestimate the real slope.

The prediction of the early sound is influenced, as can be observed in Fig. 10, by a larger spread of the measured values (especially near the source). Furthermore, the growth with distance of the early interval gives rise to decreasing or increasing trends depending on the intensity of the very early reflections. In fact, when these reflections are weak the early level tends to grow as a function of the distance [Fig. 10(a)],

TABLE VI. Relationship between measured and calculated values (according to modified theory) of the early and late sound assuming t_R as the early–late limit. Mean level differences, rms error, and slope differences between measured and theoretical values at 1 kHz frequency band.

	Mean (dB)		rms error (dB)		Slope (dB/10 m)	
Church	Early	Late	Early	Late	Early	Late
St. Sabina Basilica, Rome	1.32	0.33	2.13	0.54	0.46	−0.19
St. Apollinare in Classe, Ravenna	1.05	−0.14	1.49	0.54	0.72	−0.58
Duomo of Modena	−1.17	−0.22	1.88	0.57	−1.29	−0.60
St. Nicholas Basilica, Bari	−1.59	−0.87	1.75	0.97	−0.55	−0.33
St. Petronius Basilica, Bologna	0.97	0.53	1.50	0.73	0.66	−0.28
Lucera Cathedral	−1.28	0.10	1.53	0.33	0.38	−0.20
San Lorenzo Basilica, Florence	−0.74	−0.22	1.09	0.40	0.50	−0.11
The Holy Name of Jesus Church, Rome	−0.59	0.16	1.10	0.87	−0.21	−0.66
St. Luca and Martina, Rome	0.24	0.43	1.15	0.52	0.94	−0.36
St. Martin Basilica, Martina Franca	−0.39	−0.51	1.14	0.54	0.43	−0.30
Concattedrale, Taranto	−0.30	−0.23	0.62	0.45	−0.37	−0.54
S. Maria Assunta Church, Riola	0.33	−0.02	1.21	0.43	−0.41	−0.78
Mean	−0.18	−0.05	1.38	0.57	0.10	−0.41

TABLE VII. Relationship between measured and theoretical values of sound strength based on linear regression with source–receiver distance. Mean level differences, JND error, rms error, and slope differences between measured and theoretical values at 1 kHz frequency band.

Church	Mean (dB)		JND		rms error (dB)		Slope (dB/10 m)	
	Revised	Modified	Revised	Modified	Revised	Modified	Revised	Modified
S. Sabina Basilica, Rome	0.8	0.4	0.9	0.6	1.1	0.7	−0.38	−0.12
St. Apollinare in Classe, Ravenna	0.3	−0.1	0.6	0.4	0.7	0.4	−0.72	−0.40
Modena Cathedral	0.1	−0.3	0.7	0.5	0.9	0.7	−1.15	−0.68
St. Nicholas Basilica, Bari	0.7	−0.2	0.9	0.3	1.0	0.4	−0.81	−0.29
St. Petronius Basilica, Bologna	0.9	0.6	1.1	0.7	1.2	0.8	−0.55	−0.13
Lucera Cathedral	1.2	−0.1	1.2	0.3	1.4	0.4	−0.53	0.11
San Lorenzo Basilica, Florence	0.2	−0.4	0.5	0.4	0.7	0.5	−0.54	−0.05
The Holy Name of Jesus Church, Rome	1.2	0.1	1.6	0.5	1.8	0.7	−1.09	−0.38
St. Luca and Martina, Rome	0.9	0.2	1.1	0.5	1.2	0.5	−1.66	−0.52
St. Martin Basilica, Martina Franca	0.0	−0.5	0.5	0.6	0.6	0.6	−0.76	−0.23
Concattedrale, Taranto	0.7	−0.2	1.0	0.4	1.2	0.5	−1.44	−0.55
S. Maria Assunta Church, Riola	0.2	0.0	0.4	0.4	0.5	0.4	−0.99	−0.80
Mean	0.6	−0.1	0.9	0.4	1.0	0.6	−0.88	−0.34

while when the reflections are strong the level decreases with the distance [Fig. 10(b)]. It is interesting to observe that the new model follows the different behavior with reasonable accuracy as shown by the values of the slope difference that are generally below 1.0 dB/10 m. The rms error is higher, as could be expected due to the scatter of the measured values, but, on average, it is 1.38 dB. The largest differences are observed in churches where the mean values are also significantly different, suggesting a constant difference which could be explained by some strong early reflections not accounted for by the model.

B. Sound strength

As stated earlier, the prediction of the total sound level, or of the strength G, which is the same, was acceptable even when the classical revised theory was used. The mean predicted values were in good agreement with the measured values even though the slope was systematically underestimated, providing significant discrepancies at points far from the source. Table VII reports the results of the four accuracy indices calculated in each church with both models. The improvement brought by the new model is significant from all points of view (Fig. 12). The difference between mean values is generally below 0.5 dB. Similarly, also the mean JND is always lower than one unit, showing that the model could be used for individual position prediction. The same result is given by the rms error which is always below 1 dB, nearly halving the error obtained using Barron's model. The slope predicted using the proposed model is generally underestimated (it is slightly overestimated in only two cases), but the difference with the measured value is reduced, on average, to one-third of the value obtained using the classical revised theory.

C. Clarity index

The clarity index depends largely on the early energy level, so the new model is expected to improve the prediction accuracy. Table VIII confirms this, showing that all the indices are considerably improved when the new model is used. The difference between mean values is generally below 0.5 dB with two exceptions: St. Petronius and The Holy Name of Jesus, where the difference is about 2 dB. Both these churches show similar values even for JND and for the rms error, even though the other churches show much better values below one unit for JND and of about 1 dB for the rms error, reducing, on average, the error to one-third of the value obtained using the classical revised theory. The slope is also predicted with good accuracy independent of the church considered. The bad behavior shown by the two aforesaid churches can be related to their dimensions. In fact, they are the longest churches and the largest differences are observed at the farthest points from the sources where, apparently, the clarity assumes values as low as −15 dB because useful reflections are strongly attenuated (Fig. 12). In the church of The Holy Name of Jesus it is possible to observe a slight rise in the clarity possibly due to reflections from the back wall, as seems to be confirmed by the plateau observed in the plot of the T_S values as a function of the distance.

D. Center time

Center time is an acoustic parameter which is more suitable than clarity to check the reliability of the model. In fact, a single reflection arriving at about 80 ms could make quite a difference to the index, depending on which side of the boundary it falls. Clear evidence of this is given by the large scatter shown for clarity values (Fig. 12). On the contrary center time is less influenced by single reflections and consequently is more stable, less scattered, and, above all, is more suited to checking a model where single early reflections are schematized by a continuous function.

The analysis of the results related to the center time shows (Table IX) an astonishing improvement in the prediction of the mean values which, in most cases, are reduced to one-tenth of the value obtained using Barron's model. The slope, which was systematically underestimated by the old method, is now predicted with better accuracy. Lucera cathedral shows comparable slope differences, although of oppo-

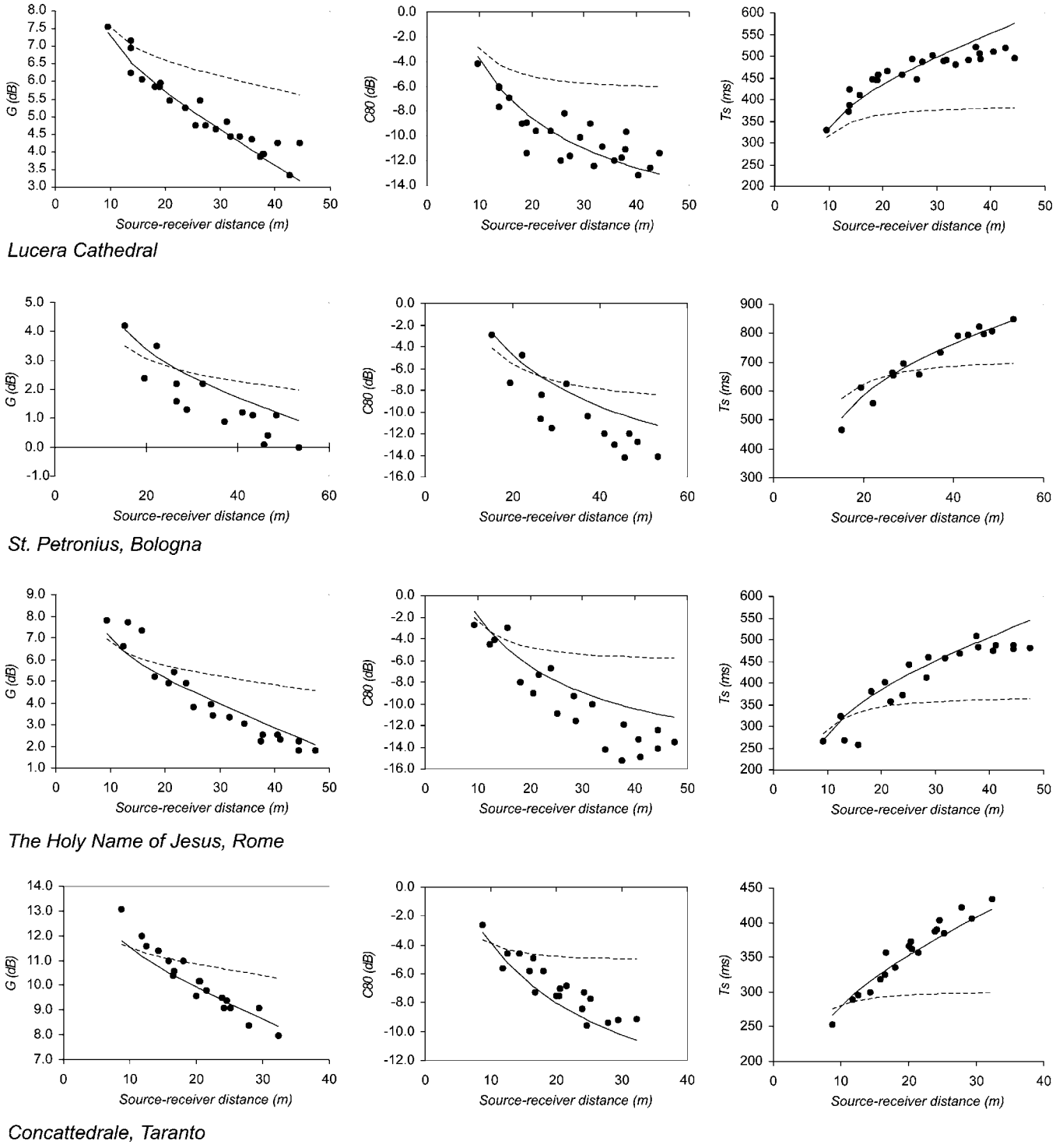

FIG. 12. Plot of measured (●) and predicted values of the strength (left), clarity (center), and center time (right) index at 1 kHz vs source–receiver distance according to the revised theory (---) and the modified theory (—).

site sign, due to lower T_S values observed at the farthest points. So, as was observed in Jesus Church, also in this case the back wall may have provided some early reflections. The analysis of rms errors shows that, on average, the discrepancy between measured and predicted values is of about 20 ms, which, on average, corresponds to an error smaller than 5% of the measured value. The largest error is observed, again, in the Holy Name of Jesus, where the error is 37 ms, corresponding to an average error of 9% of the measured values. But, as explained in Sec. VI C, this behavior mostly depends on the farthest points which are influenced by early reflections coming from the back wall.

The mean JND error is about 1.9 units, with a minimum of 0.9 and a maximum of 2.90 (observed in the Holy Name of Jesus), which would suggest the new model should not be used to calculate individual position values. However it is worth observing that the JND for center time is just 10 ms, but this value was derived[17] using an artificial system that

TABLE VIII. Relationship between measured and theoretical values of clarity based on linear regression with source–receiver distance. Mean level differences, JND error, rms error, and slope differences between measured and theoretical values at 1 kHz frequency band.

	Mean (dB)		JND		rms error (dB)		Slope (dB/10 m)	
Church	Revised	Modified	Revised	Modified	Revised	Modified	Revised	Modified
S. Sabina Basilica, Rome	2.7	−0.6	2.7	1.1	3.1	1.4	−1.24	0.28
St. Apollinare in Classe, Ravenna	2.0	0.5	2.0	0.9	2.2	1.0	−0.51	0.97
Modena Cathedral	2.2	0.2	2.6	1.0	3.1	1.2	−2.76	−0.39
St. Nicholas Basilica, Bari	3.5	0.4	3.5	0.8	3.9	1.1	−1.51	0.36
St. Petronius Basilica, Bologna	2.9	2.0	3.3	2.2	3.7	2.5	−1.57	−0.43
Lucera Cathedral	4.5	0.0	4.5	1.0	4.8	1.3	−1.15	0.66
San Lorenzo Basilica, Florence	1.9	−0.6	2.3	1.2	2.6	1.3	−1.32	0.57
The Holy Name of Jesus Church, Rome	4.8	1.9	5.0	2.1	5.8	2.5	−2.39	−0.80
St. Luca and Martina, Rome	1.8	−0.4	2.1	0.8	2.7	0.9	−4.04	−0.43
St. Martin Basilica, Martina Franca	2.6	−0.1	2.9	0.9	3.4	1.2	−3.00	−0.37
Concattedrale, Taranto	2.3	−0.9	2.4	1.0	2.8	1.1	−2.30	0.29
S. Maria Assunta Church, Riola	0.9	−0.1	1.3	0.7	1.6	0.8	−2.30	−0.95
Mean	2.7	0.2	2.9	1.1	3.3	1.4	−2.01	−0.02

simulated an "average" concert hall with 2 s reverberation time and a clarity index of 3 dB. The JND proved to be motif-dependent so that a slower and legato motif gave a longer limen (11.4±2.7 s) so it is reasonable to suppose that in churches having an average T of 5 s the difference limen for center time would be longer than 10 ms. If it were only doubled, the actual JND error could be halved, meaning that the prediction would be reliable in most of the churches. However, a visual inspection of Fig. 12 confirms the good agreement between predictions made using the proposed model and measurements.

VII. CONCLUSIONS

A sample of twelve churches was surveyed in order to investigate how sound propagates in this kind of complex space. The churches chosen differed in size (from 5500 to 160 000 m^3), in architectural style (from Early-Christian to Modern), and in typology (basilica, central, cruciform, and so on), in order to provide a representative sample. All the churches were analyzed in unoccupied conditions by using two source positions and an average of nine receivers.

The analysis of the measurements showed that the sound in churches propagates following complex paths so that, in most of the cases, the early reflections reach the farthest points with a negligible energy content. In fact, the relative sound level decreases as a function of the distance, as happens in concert halls and other proportionate spaces, but the rate of decrease is significantly steeper in churches.

The analysis of early and late reflected energy showed that the observed behavior mostly depends on the early part. In particular, it appeared that different architectural elements (such as columns, chapels, vaults, roofs, and so on) affect the early reflections so that their intensity and their density is reduced in a way that makes the purely exponential sound decay start with a significant delay after the direct sound arrival. In particular deep side chapels appear to reflect the sound according to complex paths, while side aisles and

TABLE IX. Relationship between measured and theoretical values of center time based on linear regression with source–receiver distance. Mean level differences, JND error, rms error, and slope differences between measured and theoretical values at 1 kHz frequency band.

	Mean (ms)		JND error		rms error (ms)		Slope (ms/10 m)	
Church	Revised	Modified	Revised	Modified	Revised	Modified	Revised	Modified
S. Sabina Basilica, Rome	−33	−6	3.8	1.9	43	21	21.6	4.12
St. Apollinare in Classe, Ravenna	−29	−7	3.0	0.9	35	14	25.5	7.7
Modena Cathedral	−27	5	4.6	2.4	55	31	64.2	28.1
St. Nicholas Basilica, Bari	−71	−16	7.2	2.0	80	24	34.1	−0.8
St. Petronius Basilica, Bologna	−42	5	7.3	2.1	88	27	63.7	6.3
Lucera Cathedral	−96	9	9.6	2.5	102	31	28.0	−23.9
San Lorenzo Basilica, Florence	−58	13	7.7	2.1	89	25	58.5	1.0
The Holy Name of Jesus Church, Rome	−66	20	8.0	2.9	91	37	47.4	−4.4
St. Luca and Martina, Rome	−21	10	3.0	1.3	35	18	53.8	1.7
St. Martin Basilica, Martina Franca	−52	3	5.9	2.0	67	27	51.6	−5.4
Concattedrale, Taranto	−63	−5	6.5	1.2	76	14	67.7	13.2
S. Maria Assunta Church, Riola	−12	4	2.7	1.9	32	23	50.7	32.0
Mean	−47	3	5.8	1.9	66	24	47.2	5.0

decorated walls reduce the lateral reflections, making them weaker and scattered. Trussed roofs and highly diffusing ceilings show similar behavior, while vaults, especially barrel vaults, provide stronger reflections.

A more detailed analysis of the onset time t_R of the reverberant sound field as a function of the distance showed that it grows with the source–receiver distance and it can be reasonably assumed to be proportional to the direct sound delay t_D. The analysis of the ratios t_R/t_D showed that similar values were found in similar churches.

All these results were then used in order to refine a prediction model previously tested only in Apulian-Romanesque churches. In particular, simpler rules to assign the parameters ρ and s (an aspect which was quite critical in the first formulation) were proposed as a function of the architectural characteristics of the rooms.

Finally, the refined model was applied to the churches surveyed. The input parameters were derived from the geometry (V,S,r), from the reverberation time measurements (T,α), or were estimated according to the proposed classifications (s,ρ). Strength, clarity, and center time were calculated and compared with both Barron's theory and our measured values in order to check the reliability of the modified theory. The results were investigated in the terms of difference between mean values, mean rms error, mean JND error, and slope difference. The proposed model predicted relative sound level values with good accuracy. The JND error was always below one unit, with a mean value of 0.4, nearly halving the error given by the revised theory. Clarity was predicted with less accuracy, mostly because measured values (that are influenced by single reflections) are more scattered than strength. The mean JND error was 1.1 units, but it is remarkable that this value is nearly one-third of the error obtained using Barron's model. The prediction of the center time was, apparently, less accurate than the others, with the JND error being 1.9 units. However, it is strongly dependent on the difference limen for center time which is likely to be longer than 10 ms in such large reverberant spaces. In any case, the error is less than one-third of the error given by the revised theory and, for most churches, it corresponds to a difference of about 5% of the measured value.

In conclusion, the proposed relations proved to be a simple instrument to predict energy parameters in churches. Even though measured parameters are scattered due to individual position characteristics, it is significant that the model manages to predict both mean values and the slope with good accuracy.

ACKNOWLEDGMENTS

This study has been carried out within the national interest program of scientific research "*The acoustic of spaces for music*," funded by the Italian Ministry of Instruction and University Research. The authors wish to thank all the parish priests and church management for allowing access to their churches. Special thanks are due to Bengt-Inge Dalembäk and Stephen Chiles for their precious comments and their kind collaboration in reviewing this paper. The authors are finally grateful to the technicians Michele D'Alba and Francesco Settembrini for their valuable cooperation during all phases of the survey.

[1]H. Kuttruff, *Room Acoustics*, 3rd ed. (E & FN Spon, London, 1991).
[2]L. Cremer and H. A. Muller, *Principles and Applications of Room Acoustics* (Applied Science, London, 1982), Vol. **1**.
[3]M. Hodgson, "When is diffuse-field theory applicable?" Appl. Acoust. **49**, 197–207 (1996).
[4]M. Barron and L. J. Lee, "Energy relations in concert auditoriums. I," J. Acoust. Soc. Am. **84**, 618–628 (1988).
[5]S. Chiles and M. Barron, "Sound level distribution and scatter in proportionate spaces," J. Acoust. Soc. Am. **116**, 1585–1595 (2004).
[6]M. Vorlander, "Revised relation between the sound power and the average sound pressure level in rooms and consequences for acoustic measurements," Acustica **81**, 332–343 (1995).
[7]J. J. Sendra, T. Zamarreño, and J. Navarro, "Acoustics in churches," in *Computational Acoustics in Architecture*, edited by J. J. Sendra (Computational Mechanics, Southampton, 1999), pp. 133–177.
[8]M. Galindo, T. Zamarreño, and S. Giron, "Clarity and definition in Mudejar-Gothic Churches," Build. Acoust. **6**, 1–16 (1999).
[9]N. Prodi, M. Marsilio, and R. Pompoli, "On the prediction of reverberation time and strength in mosques," in Proceedings of the 17th ICA, Rome, 2001.
[10]E. Cirillo and F. Martellotta, "An improved model to predict energy-based acoustic parameters in Apulian-Romanesque churches," Appl. Acoust. **64**, 1–23 (2003).
[11]A. Magrini and P. Ricciardi, "Churches as auditoria: Analysis of acoustical parameters for a better understanding of sound quality," Build. Acoust. **10**, 135–158 (2003).
[12]E. Cirillo and F. Martellotta, "Acoustics of Apulian-Romanesque churches: Correlations between architectural and acoustic parameters," Build. Acoust. **10**, 55–76 (2003).
[13]A. P. O. Carvalho, "Relationship between objective acoustical measures and architectural features in churches," Proceedings of the W. C. Sabine Centennial Symposium, 127th Acoustical Society of America Meeting, Cambridge, MA, 1994, pp. 311–314.
[14]S. Müller and P. Massarani, "Transfer-function measurement with sweeps," J. Audio Eng. Soc. **49**, 443–471 (2001).
[15]ISO-3382, "Acoustics–Measurement of the reverberation time of rooms with reference to other acoustical parameters," ISO, Geneva, Switzerland, 1997.
[16]B. N. Gover, J. G. Ryan, and M. R. Stinson, "Measurements of directional properties of reverberant sound fields in rooms using a spherical microphone array," J. Acoust. Soc. Am. **116**, 2138–2148 (2004).
[17]T. J. Cox, W. J. Davies, and Y. W. Lam, "The sensitivity of listeners to early sound field changes in auditoria," Acustica **79**, 27–41 (1993).
[18]I. Bork, "A comparison of room simulation software—The 2nd round robin on room acoustical computer simulation," Acust. Acta Acust. 86, 943–956 (2000).